Laser Ablation Sample Transfer for Mass Spectrometry Imaging

ARTICLE *in* METHODS IN MOLECULAR BIOLOGY · JANUARY 2015

Impact Factor: 1.29 · DOI: 10.1007/978-1-4939-1357-2_13 · Source: PubMed

2 AUTHORS:

Sung-Gun Park

University of Washington Seattle

11 PUBLICATIONS **99** CITATIONS

SEE PROFILE

Kermit K Murray

Louisiana State University

132 PUBLICATIONS **2,848** CITATIONS

SEE PROFILE

analytical chemistry

Article

pubs.acs.org/ac

Infrared Laser Ablation Sample Transfer for MALDI Imaging

Sung-Gun Park and Kermit K. Murray*

Department of Chemistry, Louisiana State University, Baton Rouge, Louisiana, 70803, United States

ABSTRACT: An infrared laser was used to ablate material from tissue sections under ambient conditions for direct collection on a matrix assisted laser desorption ionization (MALDI) target. A 10 μm thick tissue sample was placed on a microscope slide and was mounted tissue-side down between 70 and 450 μm from a second microscope slide. The two slides were mounted on a translation stage, and the tissue was scanned in two dimensions under a focused mid-infrared (IR) laser beam to transfer material to the target slide via ablation. After the material was transferred to the target slide, it was analyzed using MALDI imaging using a tandem time-of-flight mass spectrometer. Images were obtained from peptide standards for initial optimization of the system and from mouse brain tissue sections using deposition either onto a matrix precoated target or with matrix addition after sample transfer and compared with those from standard MALDI mass spectrometry imaging. The spatial resolution of the transferred material is approximately 400 μm. Laser ablation sample transfer provides several new capabilities not possible with conventional MALDI imaging including (1) ambient sampling for MALDI imaging, (2) area to spot concentration of ablated material, (3) collection of material for multiple imaging analyses, and (4) direct collection onto nanostructure assisted laser desorption ionization (NALDI) targets without blotting or ultrathin sections.

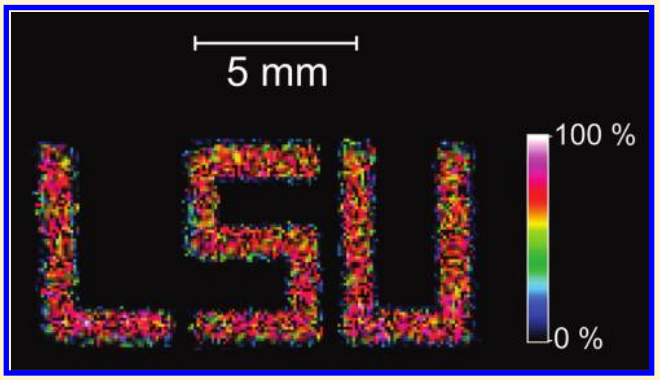

Imaging mass spectrometry using matrix assisted laser desorption ionization (MALDI) has seen rapid growth since its introduction nearly 15 years ago.[1] MALDI imaging has been primarily applied to the analysis of biomolecules in tissue sections and has been used to investigate small molecules such as pharmaceuticals and their metabolites as well as large biomolecules such as proteins.[2−5] In a MALDI imaging experiment, the tissue of interest is cut into an approximately 10 μm thick section that is deposited on a conductive microscope slide. The matrix is added by dropping, spraying, or other means, and the slide is mounted in a specially designed slide holder for insertion into the vacuum of the mass spectrometer. The image is obtained by recording mass spectra at an array of evenly spaced positions on the slide and displaying the signal intensity for an ion of a particular mass as a function of the position. The spatial resolution is limited by the spot size of the focused laser to approximately 25 μm. Higher spatial resolution can be achieved using specially designed microprobe[6] or near field optics,[7] but such approaches have not been adapted to commercial instruments. The throughput requirements of MALDI imaging have prompted a move from the 337 nm nitrogen laser to solid state lasers such as the frequency tripled Nd:YAG lasers operating at 355 nm wavelength.[8] Current commercial instruments currently operate with 1 kHz repetition rate lasers.

One of the most critical components of MALDI imaging is the addition of the matrix to the tissue sample.[9] The matrix must be applied in such a way as to promote the cocrystallization with the analyte molecules in the tissue while at the same time maintaining the lateral localization of the analyte to preserve the spatial resolution in the resulting image. The deposition of individual matrix droplets, either manually or with an automated spotter, is adequate for coarse resolution imaging, known as "profiling mode".[10] A pneumatic spray such as that from a thin layer chromatography (TLC) sprayer can produce excellent matrix and analyte interaction while at the same time good spatial resolution ("imaging mode").[11] Dry powder matrix addition is particularly effective for matrix and analtye materials that are not soluble in standard solvents,[12] and sublimation addition of matrix is another solvent-free method for MALDI imaging.[13] Imaging can also be performed on nanostructured targets. A nanostructured porous silicon DIOS target was used for imaging of 50 nm thick tissue sections.[14] The extremely thin sections were necessary to avoid covering the nanostructures with tissue. An alternate approach is to blot the tissue onto the surface and then remove it for analysis. Imaging of lipids blotted onto a commercial nanostructure assisted laser desorption ionization (NALDI) target has been reported.[15]

Although imaging using a conventional MALDI mass spectrometer is a powerful tool, there are advantages to imaging under ambient conditions, which can be accomplished with a number of ambient ionization methods.[16−21] MALDI itself can be performed under ambient conditions, which

Received: December 15, 2011
Accepted: March 12, 2012
Published: March 12, 2012

   dx.doi.org/10.1021/ac3006704 | *Anal. Chem.* 2012, 84, 3240−3245

obviates the need to deliver the sample to vacuum but still requires the addition of matrix.[22] With desorption electrospray ionization, a spray of charged droplets is directed at the sample to extract analyte that is subsequently removed and ionized. Imaging is accomplished by scanning the spray across the tissue.[23] With a surface sampling probe, the material is extracted directly from the surface for electrospray ionization.[24] Lasers can be used to ablate material that interacts with the electrospray plume for ionization, for example, in electrospray laser desorption ionization (ELDI)[25] and matrix-assisted laser desorption electrospray ionization (MALDESI).[26] Infrared lasers are highly efficient at material removal by ablation and have been used to some advantage in laser ablation based ambient ionization methods.[27−30] Laser ablation can also been used to assist surface sampling with either MALDI[31] or electrospray ionization.[32,33]

We have recently developed an ambient laser ablation sampling technique where an infrared laser is used to ablate material that is captured in a solvent droplet for subsequent mass spectrometry analysis.[34] The pulsed mid-infrared (IR) laser is tuned to the OH stretch absorption that efficiently ablates large biomolecules with little fragmentation.[35] Here, we report on the adaptation of IR laser ablation sample transfer to MALDI tissue imaging. The IR laser was used in transmission mode to ablate material from a microscope slide for capture on a second slide a fraction of a millimeter away. The approach was optimized using deposits of peptide mass standards and demonstrated with mouse brain tissue sections. The ability to sample under ambient conditions and image under vacuum was demonstrated. We also report on direct transfer to a NALDI target for imaging, multiple transfers from a single tissue section, and sample concentration by ablation from a large area onto a single target spot.

EXPERIMENTAL SECTION

Infrared laser sample transfer has been demonstrated previously with capture in a solvent droplet.[34] This approach was adapted to laser ablation sample transfer from a tissue sample to a MALDI target as shown in Figure 1. This system consisted of two indium tin oxide (ITO) coated microscope slides (259387, Bruker Daltonics, Billerica, MA, USA) that were mounted on a two-dimensional translation stage (M-433, Newport, Irvine, California) operated using computer-driven actuators (LTA-HS, Newport) and a motion controller (ESP300, Newport).

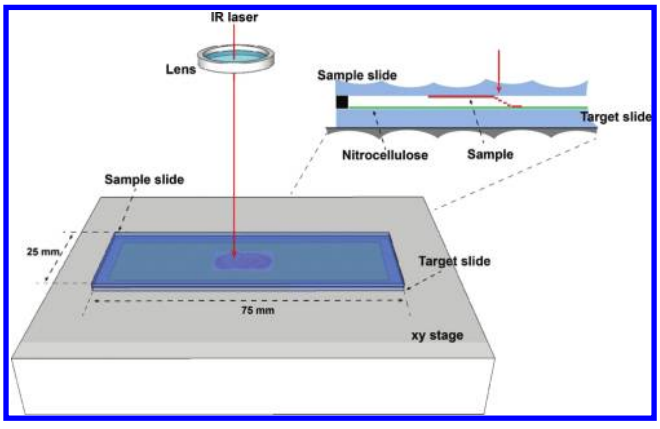

Figure 1. Schematic of the laser ablation sample transfer system for MALDI imaging.

The sample was deposited or tissue section mounted on one microscope slide (sample slide) that was placed against a second slide (target slide) or a NALDI target. The sample side faced downward toward the target, and the gap between the slide and target was adjusted using different thicknesses of adhesive tape; the spacing was determined using a measuring microscope. Thicknesses of 450, 120, and 70 μm were achieved.

The MALDI target was coated with a thin layer of nitrocellulose by spraying a solution of nitrocellulose in a methanol and acetone 4:1 (v/v) solvent using a TLC sprayer (Z529737, Sigma-Aldrich, St. Louis, Missouri). For matrix precoated targets, either 2,5-dihydroxybenzoic acid (DHB) or sinapinic acid (SA), used for mouse brain tissue imaging, or α-cyano-4-hydroxycinnamic acid (CCA), used for angiotensin II, were sprayed onto the MALDI target after the nitrocellulose. Ten coats each of the nitrocellulose and matrix solutions were applied using a 20 s spray coating followed by a 2 min interval for drying.

Samples were ablated in transmission geometry using a wavelength tunable pulsed infrared optical parametric oscillator (OPOTEK, Carlsbad, CA, USA). The laser was directed at the sample target at a 90° angle and was focused onto the sample with a 50 mm focal length lens. The pulse width was 5 ns, the repetition rate was 20 Hz, and the wavelength was set at 2.94 μm to overlap with the OH stretch absorption of the analyte.[35,36] The spot size of the laser beam at the sample was approximately 300 μm × 200 μm as determined using laser burn paper. The maximum laser energy was 2.0 mJ, corresponding to a fluence of 30 kJ/m^2. The laser was attenuated internally using laser control software, and no external optical elements were used for attenuation.

The sample slide and MALDI target were scanned under the IR laser beam to transfer material from the sample slide to the MALDI target. The linear velocity of the stage was 30 μm/s, and a serpentine pattern with 20 μm raster line spacing was traced. After the transfer of the laser ablated material to the target, mass spectra were obtained using MALDI mass spectrometry.

Mass spectra were acquired using a MALDI-TOF/TOF mass spectrometer (Ultraflextreme; Bruker) in reflectron mode. Raster scans on sample surfaces were performed in imaging mode with 300 shots per sample spot with a step size of 100 μm and a laser spot size of 100 μm. Ion images were reconstituted using FlexImaging 2.0 software (Bruker).

The peptide standard angiotensin II, reagents trifluoroacetic acid (TFA) and acetone, and matrix compounds CCA, DHB, and SA were obtained from Sigma-Aldrich (St. Louis, Missouri) and used without further purification. Nitrocellulose was purchased from Schleicher & Schuell (Dassel, Germany). HPLC grade methanol, acetonitrile (ACN), and glycerol were purchased from Fisher Scientific (Pittsburgh, Pennsylvania). House ultrapure water (18 MV cm, Barnstead E-pure System; Dubuque, Iowa) was used. A 1 mM solution of angiotensin II was prepared by dissolving in 1:1 (v/v) methanol and 0.1% aqueous TFA. A saturated matrix solution for the angiotensin II was prepared by dissolving 50 mg/mL of CCA in a 1:1 (v/v) mixture of methanol and 0.1% aqueous TFA. The matrix solution for the mouse brain tissue was prepared by dissolving 35 mg/mL of DHB in a 1:1 (v/v) mixture of methanol and 0.1% aqueous TFA. The SA matrix was dissolved in ACN and 0.2% TFA at 3:2 (v/v). The nitrocellulose solution was prepared by dissolving 100 mg in a 20 mL methanol and acetone solution at 4:1 (v/v). A glycerol solution was prepared

dx.doi.org/10.1021/ac3006704 | Anal. Chem. 2012, 84, 3240−3245

by dissolving glycerol in methanol and 0.1% aqueous TFA mixture solution in 1:1 (v/v) ratio.

Mouse brain tissue donated by the LSU School of Veterinary Medicine was stored at −80 °C until it was sliced into 10 μm thick sections using a cryostat (CM 3050; Leica Microsystems, Wetzlar, Germany). The tissue was thaw-mounted onto conductive ITO coated glass slides (Bruker). The slides were stored at −80 °C until analysis.

RESULT AND DISCUSSION

For initial tests, two MALDI targets were prepared to collect the laser-ablated material: one was coated with nitrocellulose and the other was untreated. A 2 μL volume of a 1 mM angiotensin II in 1:1 (v/v) methanol and 0.1% aqueous TFA was deposited on a microscope slide. The slide was mounted 450 μm from either the nitrocellulose coated or uncoated target microscope slide. A single spot on the sample slide was irradiated with 300 shots of 0.5 mJ of focused laser energy at 2.94 μm laser wavelength. After laser ablation sample transfer, CCA matrix was sprayed on both of the nitrocellulose coated and uncoated target slides to which the peptide had been transferred and both slides were analyzed with MALDI mass spectrometry. Figure 2a shows the mass spectrum obtained

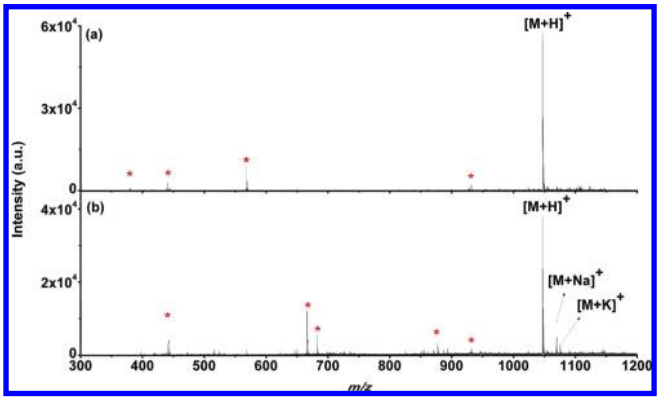

Figure 2. MALDI mass spectra of angiotensin II with infrared laser ablation sample transfer to a conductive slide coated (a) with nitrocellulose and (b) without nitrocellulose. Matrix peaks are indicated with asterisks.

from the nitrocellulose-coated target slide, and Figure 2b shows the mass spectrum obtained from the uncoated target slide. The spectra contain matrix ions (indicated with asterisks), the protonated peptide molecule, $[M + H]^+$, and alkali adduct ions. The abundance of the peptide $[M + H]^+$ ion, whether obtained from peak height or peak area, is greater with nitrocellulose. Additionally, the alkali adduct peaks are less intense. This may result from the nitrocellulose binding alkali metal impurities, thereby reducing the abundance of peptide adduct ions, resulting in enhancement of the $[M + H]^+$ ion signal.[37]

In order to gauge the dispersion of material upon laser ablation, the laser energy and slide spacing were varied and images of peptide transfer were obtained. For this experiment, a 1 mM solution of angiotensin II was sprayed on a sample target. After air-drying, a glycerol solution was sprayed over the sample slide to assist the IR laser ablation. The slide was irradiated at a single spot at laser fluences of 3, 8, and 13 kJ/m^2 at a distance of 450 μm and at distances of 70, 120, and 450 μm using 200 shots at 20 Hz repetition rate. After transfer of material from the sample slide, the target slide was spray coated with CCA matrix and imaged using MALDI. The transferred spots are shown in Figure 3 for different IR laser fluences

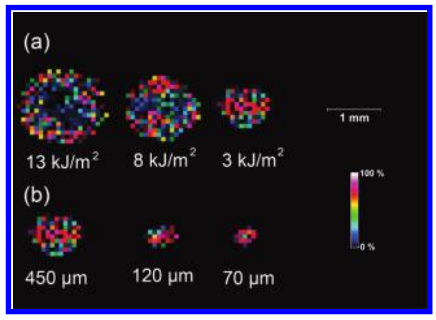

Figure 3. MALDI image of peptide spots transferred by IR laser ablation (a) at the indicated laser fluences (at a spacing of 450 μm) and (b) at the indicated slide-to-slide distances between a sample slide and a MALDI target (at a laser fluence of 3 kJ/m^2).

(Figure 3a) and different distances of the sample target from the MALDI target (Figure 3b). The spot size of the transferred material on the MALDI target is much larger than the IR laser spot size at high laser fluence (Figure 3a) and greater distance (Figure 3b). In addition, at higher IR laser fluences (8 and 13 kJ/m^2), a donut shaped image is observed. This could be due to ablation of the transferred sample or due to hydrodynamic ejection of material, which can result in removal of material from the sides of the ablation crater.[38] The size of the spot of transferred material increases with greater spacing between the slides due to the radial dispersion of the plume of ablated material. The increase in spot size with spacing in Figure 3b corresponds to an expansion angle of 110°, similar to that observed for the IR ablation of glycerol at 2.94 μm.

As a further test of the spatial resolution achievable using laser ablation sample transfer, a set of lines of peptide was transferred and imaged. For this experiment, a 1 mM solution of angiotensin II was sprayed on a microscope slide. After air-drying, a glycerol solution was sprayed over the slide. The slide was placed on top of the target with a spacing of 70 μm and irradiated with a series of single lines at 3 kJ/m^2 laser fluence. The gaps between laser ablated lines were 1 mm, 800 μm, 600 μm, 400 μm, and 300 μm. Figure 4 shows a MALDI image of the transferred lines on the target obtained with the different spacing. From this image, it can be seen that the minimum distinguishable spacing of the transferred lines on the target is 400 μm. This is well above the diffraction limit and could potentially be improved using a shorter focal length lens[32] or near field optics.[7]

Mouse brain tissue was cut into 10 μm thick sections for MALDI imaging and for laser ablation sample transfer. Two laser ablation transfers were performed: one tissue section was ablated onto a nitrocellulose-coated slide with matrix spray coated later and the other ablated onto a slide coated with both nitrocellulose and matrix. A conventional MALDI image was obtained from a section that was prepared by spraying the matrix directly onto the tissue. Mass spectra obtained from these preparations are shown in Figure 5. The slide spacing was 70 μm, and the IR laser fluence was 3 kJ/m^2. Figure 5a shows mass spectrum obtained from the matrix coated tissue section in the m/z range between 700 and 900 where phospholipids are typically detected.[39] In this spectrum, prominent ions at m/z 734.6 $[PC(32:0) + H]^+$, 756.6 $[PC(32:0) + Na]^+$, 772.6 $[PC(32:0) + K]^+$, 760.6 $[PC(34:1) + H]^+$, 782.6 [PC(34:1) +

dx.doi.org/10.1021/ac3006704 | Anal. Chem. 2012, 84, 3240−3245

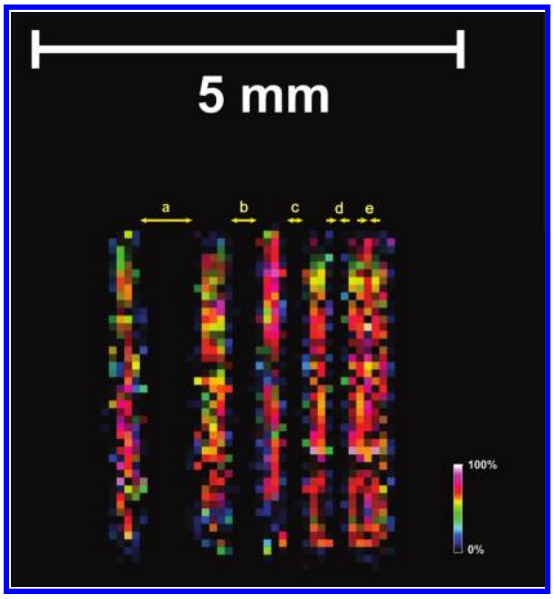

Figure 4. MALDI image of a MALDI target onto which angiotensin II peptide was transferred using an IR laser to ablate parallel lines with gaps of (a) 1 mm, (b) 800 μm, (c) 600 μm, (d) 400 μm, and (e) 300 μm.

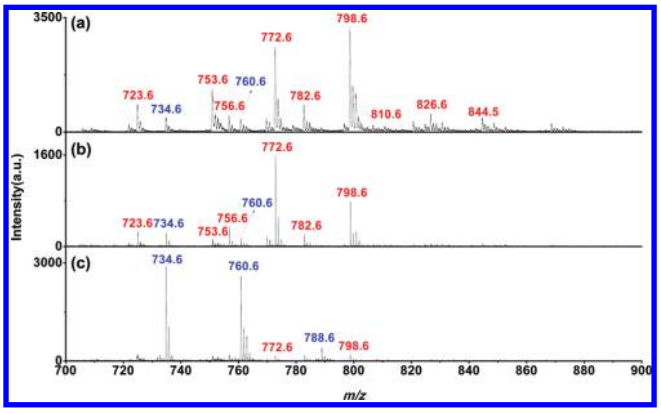

Figure 5. MALDI mass spectra of mouse brain tissue obtained by (a) standard MALDI, (b) IR laser transfer to a matrix film, and (c) IR laser transfer with subsequent matrix addition.

Na]$^+$, 798.6 [PC(34:1) + K]$^+$, 788.6 [PC(36:1) + H]$^+$, 810.6 [PC(36:1) + Na]$^+$, and 826.6 [PC(36:1) + K]$^+$ are shown.[12,40−42] Here, PC indicates phosphatidylcholine, and the numbers in parentheses indicate the alkyl chain length and number of double bonds, respectively. The mass spectra resulting from laser ablation sample transfer are comparable in intensity to the direct MALDI analysis: the signal from the matrix precoated slide is approximately half as intense (Figure 5b), and the post-transfer matrix addition yields more than 80% of the direct MALDI signal (Figure 5c). There are also fewer alkali metal adducts for the sample in which the matrix was added after the sample transfer. This is possibly a result of the partial solvation of the alkali ions and their removal through interaction with nitrocellulose. The removal of salt impurities by a nitrocellulose comatrix is a phenomenon that has been demonstrated previously.[37]

Laser ablation sample transfer can be used to concentrate material from a large area of the tissue onto a smaller region of the MALDI target. Here, the tissue slide was moved under the laser, and the target was held in place to capture the material on a single spot. Figure 6 depicts mass spectra obtained from irradiating areas of 0.3, 0.9, and 1.2 mm^2 on mouse brain tissue

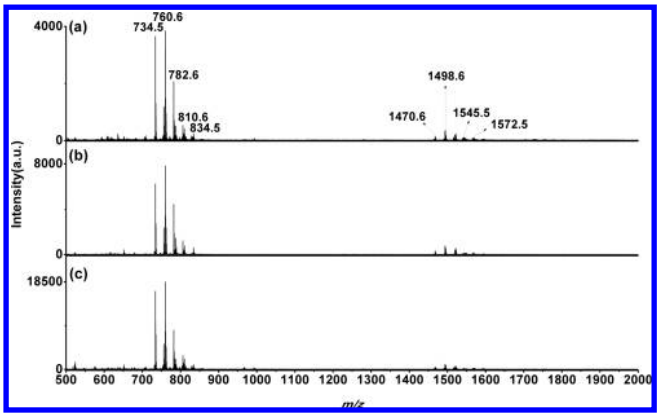

Figure 6. MALDI mass spectra obtained by area-to-spot concentration irradiating areas of (a) 0.3, (b) 0.9, and (c) 1.2 mm^2 of mouse brain tissue sections and collecting on a single spot.

sections (Figure 6a,b,c, respectively). The sections were irradiated at a slide to target spacing of 100 μm and a fluence of 3 kJ/m^2. After transfer, 2 μL of DHB matrix was added to the target that was using MALDI in reflectron mode. The spectra contain intense peaks corresponding to phospholipids in the m/z 700−900 range and peaks corresponding to gangliosides in the m/z 1400−1600 range.[43,44] The MS signal intensity increases with the irradiated area in a roughly linear fashion.

MALDI images of the mouse brain tissue prepared as tissue sections or by laser ablation sample transfer are shown in Figure 7. The sample preparation and transfer was identical to

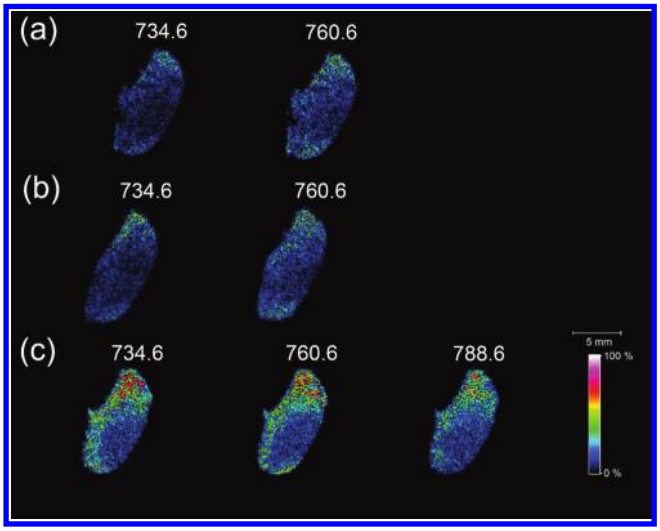

Figure 7. MALDI images of mouse brain sections (a) standard MALDI, (b) IR laser transfer to a matrix film, and (c) IR laser transfer with subsequent matrix addition.

that indicated above for Figure 5, and the prominent phosphatidylcholine peaks were used to generate the images. The spatial distribution from the mouse brain tissue with laser ablation sample preparation, both with the matrix precoated slide and post-transfer coating with matrix, is similar to that of the standard MALDI analysis.

Because the ablation sample transfer does not consume all of the tissue material, it is possible to transfer to multiple targets

dx.doi.org/10.1021/ac3006704 | *Anal. Chem.* 2012, 84, 3240−3245

for different sample preparations. To demonstrate this capability, laser ablation sample transfer from single mouse brain tissue sections was used to deposit material onto multiple targets. Figure 8 shows mass spectra and images from multiple

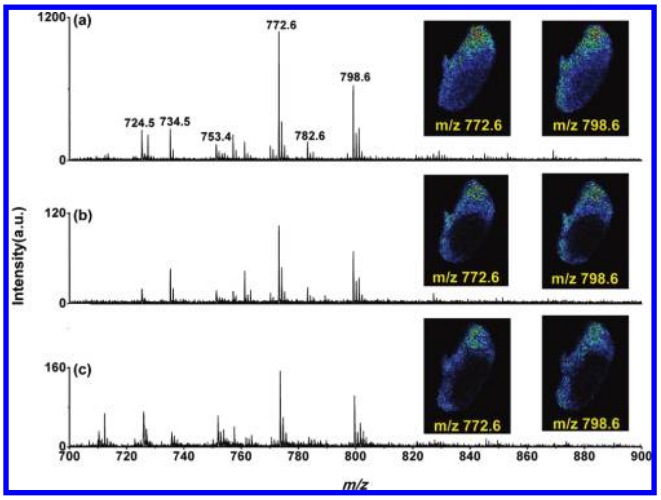

Figure 8. MALDI spectra and representative images from multiple IR laser sample transfers: (a) first transfer onto a NALDI target, (b) second transfer to a NALDI target from the same tissue section, and (c) second sample transfer to MALDI slide coated with SA matrix.

sample transfers. Figure 8a is the transfer onto a NALDI target, and Figure 8b is a second transfer to another NALDI target from the same tissue section. The sample transfer used a slide spacing of 70 μm, and IR laser fluence was 3 kJ/m^2. A 10 Hz laser repetition rate and 30 μm/s translation stage velocity was used. The spectra and images were obtained with no treatment of the NALDI target following the transfer. The signal was reduced by a factor of 10 on the second laser pass. Figure 8c was obtained from second sample transfer to a target slide coated with SA after an initial sample transfer to a target slide coated with DHB. The signal was reduced by a factor of 10 for the second laser ablation transfer MALDI run as well.

CONCLUSIONS

Ambient sampling with laser ablation sample transfer was demonstrated for MALDI imaging using a commercial TOF mass spectrometer. With a mid-infrared laser operating in the 2.94 μm wavelength region, it was possible to ablate material from a tissue section and transfer it to a microscope slide for MALDI imaging. Due to the expanding plume, the size of the transferred material increased as the distance between the two targets increased. The expanded distribution of the ablated material limited the spatial resolution to approximately 400 μm. Additionally, high energies were found to produce an uneven distribution of transferred material. The spatial distribution phospholipids from mouse brain tissue prepared by laser ablation sample transfer was similar to that of the standard MALDI imaging. Concentration of ablated material from area to spot was demonstrated, and the increase in signal was approximately linear with the area ablated. Ablation deposition onto multiple analysis targets was demonstrated with ablation onto targets coated with different matrix from the same tissue sample. Direct ablation onto nanostructured (NALDI) targets was demonstrated, eliminating the need for either ultrathin tissue sections or tissue blotting. Ongoing work is directed at improving the spatial resolution of material transfer using improved optics.

AUTHOR INFORMATION

Corresponding Author

*E-mail: kkmurray@lsu.edu.

Notes

The authors declare no competing financial interest.

ACKNOWLEDGMENTS

This work was supported by the National Science Foundation, Grant Number CHE-0848319.

REFERENCES

(1) Caprioli, R. M.; Farmer, T. B.; Gile, J. *Anal. Chem.* **1997**, *69*, 4751−4760.
(2) Stoeckli, M.; Chaurand, P.; Hallahan, D.; Caprioli, R. M. *Nat. Med.* **2001**, *7*, 493−496.
(3) Chaurand, P.; Sanders, M. E.; Jensen, R. A.; Caprioli, R. M. *Am. J. Pathol.* **2004**, *165*, 1057−1068.
(4) McDonnell, L. A.; Heeren, R. M. A. *Mass Spectrom. Rev.* **2007**, *26*, 606−643.
(5) Walch, A.; Rauser, S.; Deininger, S.-O.; Höfler, H. *Histochem. Cell Biol.* **2008**, *130*, 421−434.
(6) Guenther, S.; Koestler, M.; Schulz, O.; Spengler, B. *Int. J. Mass Spectrom.* **2010**, *294*, 7−15.
(7) Schmitz, T. A.; Gamez, G.; Setz, P. D.; Zhu, L.; Zenobi, R. *Anal. Chem.* **2008**, *80*, 6537−6544.
(8) Spraggins, J. M.; Caprioli, R. M. *J. Am. Soc. Mass Spectrom.* **2011**, *22*, 1022−1031.
(9) Bouschen, W.; Spengler, B. *Int. J. Mass Spectrom.* **2007**, *266*, 129−137.
(10) Chaurand, P.; Norris, J. L.; Cornett, D. S.; Mobley, J. A.; Caprioli, R. M. *J. Proteome Res.* **2006**, *5*, 2889−2900.
(11) Wang, H.-Y. J.; Jackson, S. N.; Post, J.; Woods, A. S. *Int. J. Mass Spectrom.* **2008**, *278*, 143−149.
(12) Puolitaival, S. M.; Burnum, K. E.; Cornett, D. S.; Caprioli, R. M. *J. Am. Soc. Mass Spectrom.* **2008**, *19*, 882−886.
(13) Hankin, J. A.; Barkley, R. M.; Murphy, R. C. *J. Am. Soc. Mass Spectrom.* **2007**, *18*, 1646−1652.
(14) Liu, Q.; Guo, Z.; He, L. *Anal. Chem.* **2007**, *79*, 3535−3541.
(15) Vidová, V.; Novák, P.; Strohalm, M.; Pól, J.; Havlícek, V.; Volný, M. *Anal. Chem.* **2010**, *82*, 4994−4997.
(16) Van Berkel, G. J.; Pasilis, S. P.; Ovchinnikova, O. *J. Mass Spectrom.* **2008**, *43*, 1161−1180.
(17) Weston, D. J. *Analyst* **2010**, *135*, 661−668.
(18) Ifa, D. R.; Wu, C.; Ouyang, Z.; Cooks, R. G. *Analyst* **2010**, *135*, 669−681.
(19) Dill, A. L.; Eberlin, L. S.; Ifa, D. R.; Cooks, R. G. *Chem. Commun.* **2011**, *47*, 2741−2746.
(20) Alberici, R. M.; Simas, R. C.; Sanvido, G. B.; Romão, W.; Lalli, P. M.; Benassi, M.; Cunha, I. B. S.; Eberlin, M. N. *Anal. Bioanal. Chem.* **2010**, *398*, 265−294.
(21) Harris, G. A.; Galhena, A. S.; Fernandez, F. M. *Anal. Chem.* **2011**, *83*, 4508−4538.
(22) Li, Y.; Shrestha, B.; Vertes, A. *Anal. Chem.* **2007**, *79*, 523−532.
(23) Wiseman, J. M.; Ifa, D. R.; Zhu, Y.; Kissinger, C. B.; Manicke, N. E.; Kissinger, P. T.; Cooks, R. G. *Proc. Natl. Acad. Sci. U.S.A* **2008**, *105*, 18120−18125.
(24) Van Berkel, G. J.; Kertesz, V.; Koeplinger, K. A.; Vavrek, M.; Kong, A.-N. T. *J. Mass Spectrom.* **2008**, *43*, 500−508.
(25) Shiea, J.; Huang, M.-Z.; Hsu, H.-J.; Lee, C.-Y.; Yuan, C.-H.; Beech, I.; Sunner, J. *Rapid Commun. Mass Spectrom.* **2005**, *19*, 3701−3704.
(26) Sampson, J. S.; Hawkridge, A. M.; Muddiman, D. C. *J. Am. Soc. Mass Spectrom.* **2006**, *17*, 1712−1716.

(27) Sampson, J. S.; Murray, K. K.; Muddiman, D. C. *J. Am. Soc. Mass Spectrom.* **2009**, *20*, 667−673.
(28) Rezenom, Y. H.; Dong, J.; Murray, K. K. *Analyst* **2008**, *133*, 226−232.
(29) Nemes, P.; Vertes, A. *Anal. Chem.* **2007**, *79*, 8098−8106.
(30) Galhena, A. S.; Harris, G. A.; Nyadong, L.; Murray, K. K.; Fernandez, F. M. *Anal. Chem.* **2010**, *82*, 2178−2181.
(31) Huang, M.-Z.; Jhang, S.-S.; Cheng, C.-N.; Cheng, S.-C.; Shiea, J. *Analyst* **2010**, *135*, 759−766.
(32) Ovchinnikova, O. S.; Kertesz, V.; Van Berkel, G. J. *Anal. Chem.* **2011**, *83*, 1874−1878.
(33) Ovchinnikova, O. S.; Kertesz, V.; Van Berkel, G. J. *Rapid Commun. Mass Spectrom.* **2011**, *25*, 3735−3740.
(34) Park, S.-G.; Murray, K. K. *J. Am. Soc. Mass Spectrom.* **2011**, *22*, 1352−1362.
(35) Little, M. W.; Laboy, J.; Murray, K. K. *J. Phys Chem. C* **2006**, *111*, 1412−1416.
(36) Caldwell, K. L.; McGarity, R. D.; Murray, K. K. *J. Mass Spectrom.* **1997**, *32*, 1374−1377.
(37) Preston, L. M.; Murray, K. K.; Russell, D. H. *Biol. Mass Spectrom.* **1993**, *22*, 544−550.
(38) Fan, X.; Murray, K. K. *J. Phys. Chem. A* **2009**, *114*, 1492−1497.
(39) Shrestha, B.; Nemes, P.; Nazarian, J.; Hathout, Y.; Hoffman, E. P.; Vertes, A. *Analyst* **2010**, *135*, 751−758.
(40) Murphy, R. C.; Hankin, J. A.; Barkley, R. M. *J. Lipid Res.* **2009**, *50* (Suppl), S317−S322.
(41) Shrivas, K.; Hayasaka, T.; Goto-Inoue, N.; Sugiura, Y.; Zaima, N.; Setou, M. *Anal. Chem.* **2010**, *82*, 8800−8806.
(42) Wang, H.; Manicke, N. E.; Yang, Q.; Zheng, L.; Shi, R.; Cooks, R. G.; Ouyang, Z. *Anal. Chem.* **2011**, *83*, 1197−1201.
(43) Goto-Inoue, N.; Hayasaka, T.; Zaima, N.; Kashiwagi, Y.; Yamamoto, M.; Nakamoto, M.; Setou, M. *J. Am. Soc. Mass. Spectrom.* **2010**, *21*, 1940−1943.
(44) Chan, K.; Lanthier, P.; Liu, X.; Sandhu, J. K.; Stanimirovic, D.; Li, J. *Anal. Chim. Acta* **2009**, *639*, 57−61.